Proceedings of the Seventeenth International Conference on
Civil, Structural and Environmental Engineering Computing
Edited by: P. Iványi, J. Kruis and B.H.V. Topping
Civil-Comp Conferences, Volume 6, Paper 9.5
Civil-Comp Press, Edinburgh, United Kingdom, 2023
doi: 10.4203/ccc.6.9.5

Bifurcation of compressible elastic cylinders under internal pressure and axial loading

S. Parikh[1] and M. Latorre[2]

**[1]Department of Biomedical Engineering
Maastricht University, Maastricht, The Netherlands**

**[2]Center for Research and Innovation in Bioengineering
Universitat Politècnica de València, València, Spain**

Abstract

A theoretical formulation for the bifurcation of pressurized and axially stretched thin-walled cylinders obeying compressible hyperelastic material law is derived. Analytical solutions are provided for three bifurcation conditions, namely prismatic, symmetric, and composite. Validation of the formulation in the incompressible limit is performed by limiting the bulk modulus towards incompressibility and comparing it against bifurcation analysis for incompressible materials analyzed in previous studies. Analytical solutions are obtained for two strain energy functions. Finite element simulations are performed for validating numerically the analytical results for compressible behavior. A stabilizing effect in the critical values of deformation is observed with an increase in the compressibility of the material.

Keywords: compressible materials, bifurcation analysis, cylindrical membrane

1 Introduction

We propose a general theory that describes the bifurcation of thin-walled (hyperelastic) cylinders which are subjected to inflation and axial stretching. Our analysis extends the theory presented by [1] to compressible materials. We describe a theoretical framework to understand the incremental deformation equations eventually leading to bifurcation conditions. Three different bifurcation conditions are studied namely prismatic, symmetric, and composite bifurcations. Numerical analysis based on finite elements (FE) is performed to validate numerically the results obtained analytically. A limiting case towards incompressibility is also analyzed.

2 General equations

The bifurcation analysis of a thin-walled cylinder is based on incremental equations which involve the superimposition of small deformations on a state which has finitely deformed [1].

2.1 Incremental motion equations

Consider a line element $d\boldsymbol{X}$ in the reference configuration β_{ref} of a deformable (hyper)elastic body. The body undergoes a deformation to attain an intermediate deformed configuration β_{int}. The line element $d\boldsymbol{X}$ is transformed to $d\boldsymbol{x}_0$ through the deformation gradient tensor $\mathbf{F}_0$. The intermediate configuration further undergoes an incremental deformation thereby producing the current deformed configuration β_{cur}. The line element $d\boldsymbol{x}_0$ is transformed to $d\boldsymbol{x}$ via the deformation gradient tensor $\boldsymbol{F}$. The total deformation gradient tensor (mapping $d\boldsymbol{X}$ to $d\boldsymbol{x}$) is $\mathbf{F} = \boldsymbol{F}\mathbf{F}_0$.

The incremental change in the line element is represented by Δdx,

$$\Delta d\boldsymbol{x} = d\boldsymbol{x} - d\boldsymbol{x}_0. \tag{1}$$

With respect to the reference configuration, Δdx can be represented as

$$\Delta d\boldsymbol{x} = \mathbf{F}d\boldsymbol{X} - \mathbf{F}_0 d\boldsymbol{X} = (\mathbf{F} - \mathbf{F}_0)d\boldsymbol{X} = \Delta\mathbf{F}d\boldsymbol{X}. \tag{2}$$

Therefore,

$$\Delta\mathbf{F} = \mathbf{F} - \mathbf{F}_0 = (\boldsymbol{F} - \mathbf{I})\mathbf{F}_0 = \Delta\boldsymbol{F}\mathbf{F}_0. \tag{3}$$

where $\mathbf{I}$ is the second-order identity tensor. $\Delta\boldsymbol{F}$ can be further represented as

$$\Delta\boldsymbol{F} = \boldsymbol{F} - \mathbf{I} = (\mathbf{I} + \nabla\boldsymbol{u}) - \mathbf{I} = \nabla\boldsymbol{u}, \tag{4}$$

with $\nabla\boldsymbol{u}$ the gradient of the (incremental) displacement field $\boldsymbol{u} = \boldsymbol{x} - \boldsymbol{x}_0$ with respect to the intermediate configuration β_{int}.

2.2 Incremental stress equations

The total nominal stress tensor ($\mathbf{N}$) is expressed in terms of the Cauchy ($\boldsymbol{\sigma}$) and second Piola-Kirchhoff ($\mathbf{S}$) stress tensors as

$$\mathbf{N} = \mathrm{J}\mathbf{F}^{-1}\boldsymbol{\sigma} = \mathbf{S}\mathbf{F}^{\mathrm{T}}, \tag{5}$$

where J is the determinant of $\mathbf{F}$.

The nominal stress tensor can be written as

$$\mathbf{N} = \mathbf{N}_0 + \Delta\mathbf{N} = \mathbf{N}_0 + \mathbf{S}_0\Delta\mathbf{F}^{\mathrm{T}} + \Delta\mathbf{S}\mathbf{F}_0^{\mathrm{T}}, \tag{6}$$

where $\mathbf{N}_0$ is the contribution to $\mathbf{N}$ from the intermediate deformed configuration, while $\Delta\mathbf{N}$ is the contribution to $\mathbf{N}$ from the incremental deformation. On further expansion of Eq 6, $\Delta\mathbf{N}$ becomes

$$\Delta\mathbf{N} = (\mathbf{S_0} \oplus \mathbf{I} + \mathbf{I} \odot \mathbf{F}_0 : \mathbb{C}_0 : \frac{1}{2}(\mathbf{F}_0^{\mathrm{T}} \odot \mathbf{I} + \mathbf{I} \oplus \mathbf{F}_0^{\mathrm{T}})) : \Delta\mathbf{F} = \mathbb{A}_0 : \Delta\mathbf{F}, \tag{7}$$

where $(\mathbf{A} \odot \mathbf{B})_{ijkl} = A_{ik}B_{jl}$ and $(\mathbf{A} \oplus \mathbf{B})_{ijkl} = A_{il}B_{jk}$ in index notation, $\Delta\mathbf{C} = \mathbf{F}_0^{\mathrm{T}}\Delta\mathbf{F} + \Delta\mathbf{F}^{\mathrm{T}}\mathbf{F}_0$ with $\mathbf{C} = \mathbf{F}^{\mathrm{T}}\mathbf{F}$ the right Cauchy–Green tensor, and $\mathbb{C} = 2\partial\mathbf{S}/\partial\mathbf{C}$ is the material fourth-order elasticity tensor. We recognize $\mathbb{A}$ as the fourth-order elasticity tensor for the work-conjugate tensors $\{\mathbf{N}, \mathbf{F}\}$ [2].

2.2.1 Incremental stress equations with respect to intermediate configuration

Consider an additive decomposition of the Cauchy stress $\boldsymbol{\sigma}$ into the "extra" part $\boldsymbol{\sigma}^x$ (i.e., that derived from the strain energy function) and a volumetric part $\boldsymbol{\sigma}_{vol}$

$$\boldsymbol{\sigma} = \boldsymbol{\sigma}^x + \boldsymbol{\sigma}_{vol} = \boldsymbol{\sigma}^x - p\mathbf{I}, \tag{8}$$

where, for convenience to obtain the incompressible limit, we represent $\boldsymbol{\sigma}_{vol}$ as $-p\mathbf{I}$ (with p the Lagrange multiplier that enforces incompressibility in that limit only). The final form for $\Delta\boldsymbol{N}$, where $\boldsymbol{N} = J\boldsymbol{F}^{-1}\boldsymbol{\sigma}$ is the nominal stress tensor with respect to the intermediate configuration, can be written as

$$\Delta\boldsymbol{N} = \mathbb{B}_0^x : \nabla\boldsymbol{u} + p_0\nabla\boldsymbol{u} - p_0\Delta J\mathbf{I} - \Delta p\mathbf{I}, \tag{9}$$

where

$$\begin{aligned} \mathbb{B}_0^x &= \mathrm{J}_0^{-1}\mathbf{F}_0 \odot \mathbf{I} : \mathbb{A}_0^x : \mathbf{I} \odot \mathbf{F}_0^{\mathrm{T}} \\ &= \boldsymbol{\sigma}_0^x \boxdot \mathbf{I} + \mathrm{J}_0^{-1}\mathbf{F}_0 \odot \mathbf{F}_0 : \mathbb{C}_0^x : \mathbf{F}_0^{\mathrm{T}} \odot \mathbf{F}_0^{\mathrm{T}} \\ &= \boldsymbol{\sigma}_0^x \boxdot \mathbf{I} + \boldsymbol{c}_0^x \end{aligned} \tag{10}$$

Note that $\boldsymbol{c} = \mathrm{J}^{-1}\mathbf{F} \odot \mathbf{F} : \mathbb{C} : \mathbf{F}^{\mathrm{T}} \odot \mathbf{F}^{\mathrm{T}}$ is the spatial fourth-order elasticity tensor.

Ultimately, Eq 9 represents the general form for the incremental nominal stress for non-linear elastic materials in the intermediate configuration. This equation is comparable to Eq 103 in [3]. Under detailed inspection, it can be concluded that Eq 103 in [3] is a case-specific equation for non-linear elastic incompressible materials. Case-specificity of Eq 103 in [3] can be justified due to the absence of term $-p_0\Delta J\mathbf{I}$ from Eq 9, since for incompressible materials $J = 1$ and $\Delta J = 0$.

3 Compressible thin-walled circular elastic cylinders

For a thin cylinder, let (r, θ, z) be the polar coordinates in the current deformed configuration, where r is the radius corresponding to the middle surface of the membrane, $0 \leq \theta \leq 2\pi$ and $0 \leq z \leq l$ (l is the deformed length of the cylinder after axial stretch λ_z). In Cartesian coordinates, let $\mathbf{a}_1$ and $\mathbf{a}_2$ be the unit basis vectors corresponding to θ and z in the current deformed configuration, and $\mathbf{a}_3$ be the unit normal vector in the outward direction to the membrane middle-surface. $\mathbf{u}$ can be written as

$$\mathbf{u} = v\mathbf{a}_1 + w\mathbf{a}_2 + u\mathbf{a}_3. \tag{11}$$

and

$$\nabla\mathbf{u} = \begin{bmatrix} \frac{1}{r}(u + v_\theta) & v_z & -\frac{1}{r}(u_\theta - v) \\ \frac{1}{r}w_\theta & w_z & -u_z \\ \frac{1}{r}(u_\theta - v) & u_z & \eta_{33} \end{bmatrix}, \tag{12}$$

where the subscript of the tensor element denotes the derivative of $\mathbf{u}$ with the particular direction in polar coordinates. Additionally, we use the notation $\eta_{ij} = \nabla u_{ij}$. The last term η_{33} is to be derived from the volumetric part of the strain energy density function.

Denoting ΔN_{ij} as Π_{ij}, the incremental equilibrium equations similar to [3] are

$$\begin{gathered} \Pi_{11,1} + \Pi_{21,2} + \frac{1}{3}\Pi_{13} - \frac{P}{h}\eta_{31} = 0 \\ \Pi_{12,1} + \Pi_{22,2} - \frac{P}{h}\eta_{32} = 0 \\ \Pi_{13,1} + \Pi_{23,2} - \frac{1}{r}\Pi_{11} + \frac{P}{h}(\eta_{11} + \eta_{22}) + \frac{\Delta P}{h} = 0. \end{gathered} \tag{13}$$

where P is the internal pressure and h is the thickness of the cylinder in the current configuration. In compact form, they are represented as

$$\begin{gathered} \Sigma_1 \frac{u_\theta + v_{\theta\theta}}{r^2} + \Sigma_2 v_{zz} + \Sigma_3 \frac{w_{\theta z}}{r} = 0 \\ \Sigma_4 \frac{u_z}{r} + \Sigma_5 \frac{v_{\theta z}}{r} + \Sigma_6 \frac{w_{\theta\theta}}{r^2} + \Sigma_7 w_{zz} = 0 \\ \Sigma_8 \frac{u}{r^2} - \Sigma_9 \frac{u_{\theta\theta}}{r^2} - \Sigma_{10} u_{zz} + \Sigma_{11} \frac{v_\theta}{r^2} + \Sigma_{12} \frac{w_z}{r} - \frac{\Delta P}{h} = 0. \end{gathered} \tag{14}$$

3.1 Prismatic bifurcations

In order for the prismatic bifurcations to occur, the dependence of v, w and u (*cf.* Eq. 11) is considered only on θ. Following the line of reasoning provided in equations 32-36 in [1] and implementing them on the given compressible material case, the prismatic bifurcation condition becomes $\Sigma_1 = 0$. However, for rubber-like solids, $\Sigma_1 > 0$ [1], which deems bifurcation impossible.

3.2 Symmetric bifurcations

Symmetric bifurcations condition is characterized by the dependence of v, w and u only on z reducing Eq 14 to

$$\begin{gathered}\Sigma_2 v_{zz} = 0 \\ \Sigma_4 u_z + \Sigma_7 r w_{zz} = 0 \\ \Sigma_8 u - \Sigma_{10} r^2 u_{zz} + (\Sigma_3 - \Sigma_2 + \Sigma_{10} - \Sigma_1 + \Sigma_{8)} r w_z = \frac{\Delta P r^2}{h}. \end{gathered} \tag{15}$$

Therefore, only w and u depend on z. The form for w and u can be assumed as

$$\begin{aligned} u(z) &= u_0 e^{\gamma z} \\ w(z) &= w_0 e^{\gamma z} \end{aligned} \tag{16}$$

The general solution of u and w becomes

$$\begin{bmatrix} u \\ w \end{bmatrix} = c_1 \begin{bmatrix} 0 \\ 1 \end{bmatrix} + c_2 \begin{bmatrix} 1 \\ -\frac{\Sigma_8 z}{\Sigma_{12} r} \end{bmatrix} + \begin{bmatrix} c_3 \\ c_4 \frac{\Sigma_4}{\Sigma_7 \hat{\nu}} \end{bmatrix} cos(\frac{\hat{\nu} z}{r}) + \begin{bmatrix} c_4 \\ -c_3 \frac{\Sigma_4}{\Sigma_7 \hat{\nu}} \end{bmatrix} sin(\frac{\hat{\nu} z}{r}), \tag{17}$$

The modes of symmetric bifurcation can be determined for a particular ratio of l/r (l is the deformed axial length and the r is the deformed mid-surface radius of the cylinder under consideration) by applying boundary conditions ($u(z=0)=0, u(z=l)=0, w(z=0)=0, w(z=l)=0$) to Eq 17, and determining a non-trivial solution.

3.3 Composite bifurcations

Dependence of u, v and w on θ and z would give rise to composite bifurcations. With $\Delta P = 0$, the form of u, v and w can be expressed as

$$\begin{aligned} u(\theta, z) &= u_0 (\cos m\theta)(e^{\gamma z}) \\ v(\theta, z) &= v_0 (\sin m\theta)(e^{\gamma z}) \\ w(\theta, z) &= w_0 (\cos m\theta)(e^{\gamma z}), \end{aligned} \tag{18}$$

The general solution for incremental displacements is

$$\begin{aligned} \begin{bmatrix} u \\ v \\ w \end{bmatrix} = \begin{bmatrix} \cos\theta & 0 & 0 \\ 0 & \sin\theta & 0 \\ 0 & 0 & \cos\theta \end{bmatrix} \Bigg(c_1 \begin{bmatrix} 1 \\ -1 \\ 0 \end{bmatrix} + c_2 r \begin{bmatrix} \frac{z}{r} \\ \frac{-z}{r} \\ -1 \end{bmatrix} + c_3 \begin{bmatrix} \alpha_1 \\ \beta_1 \\ 1 \end{bmatrix} e^{\nu_1 \frac{z}{r}} + \\ c_4 \begin{bmatrix} -\alpha_1 \\ -\beta_1 \\ 1 \end{bmatrix} e^{-\nu_1 \frac{z}{r}} + \begin{bmatrix} c_5 \alpha_2 \\ c_5 \beta_2 \\ c_6 \end{bmatrix} \cos \frac{\hat{\nu_2} z}{r} + \begin{bmatrix} -c_6 \alpha_2 \\ -c_6 \beta_2 \\ c_5 \end{bmatrix} \sin \frac{\hat{\nu_2} z}{r} \Bigg), \end{aligned} \tag{19}$$

where, $\hat{\nu_2} = i\nu_2$ and $\alpha_1, \beta_1, \alpha_2$ and β_2 are the functions of $\Sigma_1, \Sigma_2, \Sigma_3, \Sigma_4, \Sigma_5, \Sigma_7, \Sigma_{10}, \Sigma_{11}$ and Σ_{12}.

4 Numerical validation

In this section, we delineate the validation of the theory presented in this study numerically. The theory for compressible materials was implemented on two material models - neo-Hookean (Eq 20) and Ogden (Eq 21). A coupled form of the strain-energy function was considered for each material model

$$\psi = \frac{\mu}{2}(I_1 - 3 - 2\ln J) + \frac{1}{2}k(J^2 - 1) \tag{20}$$

$$\psi = \sum_{p=1}^{n} \frac{\mu_p}{\alpha_p}(\lambda_1^{\alpha_p} + \lambda_2^{\alpha_p} + \lambda_3^{\alpha_p} - \alpha_p \ln J)) + \frac{1}{2}k(J^2 - 1), \tag{21}$$

where, $n = 3$, $I_1 = tr(\mathbf{F}^{\mathrm{T}}\mathbf{F})$, μ and μ_p are the shear moduli, α_p are dimensionless constants, k represents the bulk modulus,and $\lambda_1, \lambda_2, \lambda_3$ are the stretches in the principal directions. The property $2\mu = \sum_{p=1}^{n} \mu_p \alpha_p$ holds true. For the values of shear moduli and dimensionless constants, refer to Table 1.

Table 1: Values for shear moduli and dimensionless parameters for the models

Material	μ **[MPa]**	μ_1 **[MPa]**	μ_2 **[MPa]**	μ_3 **[MPa]**	α_1 **[-]**	α_2 **[-]**	α_3 **[-]**
ne-Hookean	0.4225	-	-	-	-	-	-
Ogden	-	0.63	0.0012	-0.01	1.3	5.0	-2.0

Finite element (FE) simulations were performed in order to validate the theory presented in this study. In accordance with [4], the undeformed dimensions of the cylinder were considered as follows: inner radius $R_i = 4mm$, thickness $H = 0.2mm$, and length $L = 80mm$. A geometrical perturbation was introduced in the middle section of the cylinder by increasing the radius [$R_i(z = L/2) = 4.004$], thereby introducing a slight curvature of the cylinder along the axial length. A constant thickness was maintained throughout the length of the cylinder. The meshed cylinder consisted of 25200 hexahedral elements. The radial direction consisted of 5 elements to capture a realistic stress gradient due to radial expansion while being pressurized (pressure applied on the inner surface of the cylinder).

The cylindrical geometry was prescribed with neo-Hookean material model (for material parameters see Table 1). First, the FE model was validated against the results from a previous study ([4]; figure 6) for an incompressible case (where, $k = 1000\mu$ in Eq 20). Three axial stretches were prescribed ($\lambda_z = 1.2, 1.5, 1.8$) in order to validate the model against the analytical solution. Thereafter, the FE model was validated against the analytical solution for compressible cases (where, $k = 1\mu$ and 5μ). All simulations were performed in FEBio [5].

Similar to [4], Figure 1 indicates the validation of the analytical solution of symmetric bifurcation condition with FE analysis. The symmetric bifurcation condition is indicated by Eq 15, where $L/R = 20$ was considered (also for the FE model; sec 6.2).

The equality criterion from Eq 15 was considered to plot the monotonically decreasing analytical curves in 1.

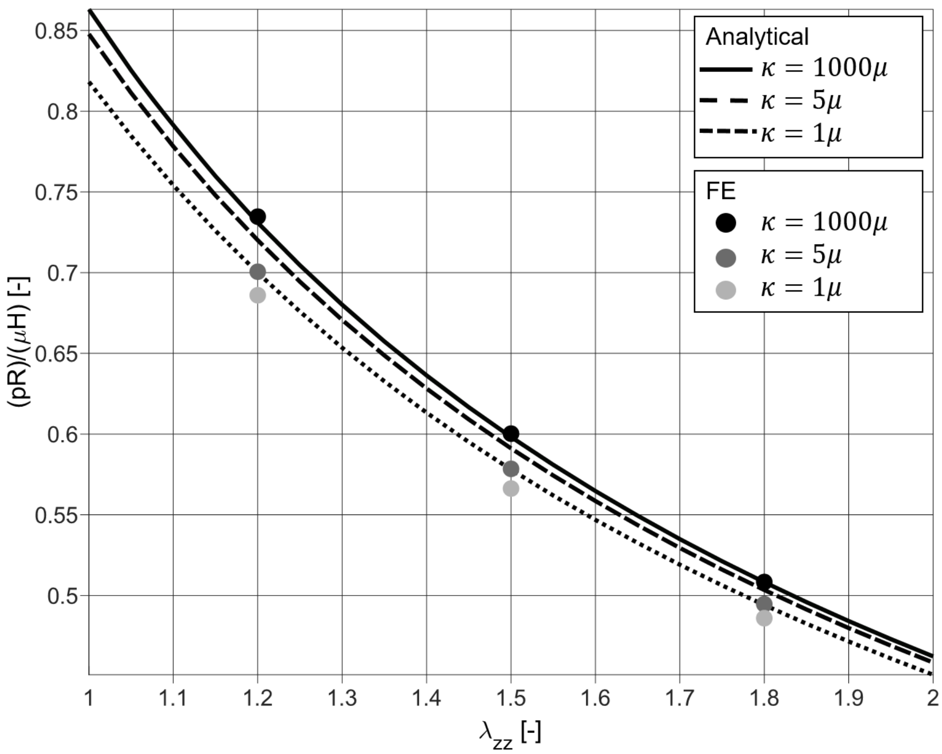

Figure 1: Normalized values of critical pressures at which symmetric bifurcation occurs for given axial stretches. Continuous curves indicate analytical solutions, while the discrete values indicate FE simulation results. The curves are for neo-Hookean material model.

5 Concluding remarks

In conclusion, by incorporating the contribution of an additional volumetric term to the incremental nominal stress tensor, we provide a formulation of bifurcation analysis for thin-walled compressible cylinders. The bifurcation behavior for compressible materials is similar to that of incompressible materials. In the limit of incompressibility ($\mu/\kappa = 0$), incompressible behavior is recovered from the bifurcation equations for the compressible case.

Acknowledgements

This study was supported by HS-BAFTA fellowship awarded to SP by CARIM School for Cardiovascular Diseases at Maastricht University. ML acknowledges the support given by the European Union "Horizon Europe" research and innovation program (Grant Agreement 101039349 — project G-CYBERHEART).

References

[1] Haughton D, Ogden R. Bifurcation of inflated circular cylinders of elastic material under axial loading—I. Membrane theory for thin-walled tubes. Journal of the Mechanics and Physics of Solids. 1979;27(3):179-212.

[2] Latorre M, Montans FJ. Stress and strain mapping tensors and general work-conjugacy in large strain continuum mechanics. Applied Mathematical Modelling. 2016;40(5-6):3938-50.

[3] Haughton D, Ogden R. On the incremental equations in non-linear elasticity—I. Membrane theory. Journal of the Mechanics and Physics of Solids. 1978;26(2):93-110.

[4] Alhayani A, Giraldo J, Rodríguez J, Merodio J. Computational modelling of bulging of inflated cylindrical shells applicable to aneurysm formation and propagation in arterial wall tissue. Finite Elements in Analysis and Design. 2013;73:20-9.

[5] Maas SA, Ellis BJ, Ateshian GA, Weiss JA. FEBio: finite elements for biomechanics. Journal of Biomechanical Engineering. 2012.